

TWENTY-FIVE YEARS OF INTERFEROMETRIC FIBER OPTIC ACOUSTIC SENSORS AT THE NAVAL RESEARCH LABORATORY

James H. Cole

Clay Kirkendall

Anthony Dandridge

Gary Cogdell

T.G. Giallorenzi

Naval Research Laboratory
Washington, D.C.

Abstract

Interferometric fiber optic acoustic sensors are based on measuring the phase change of light traveling in an optical fiber due to the strains developed in the fiber by an applied pressure. Fiber interferometry is extremely sensitive, allowing detection of periodic length variations on the order of a few hundred femtometers ($\sim 10^{-13}$ meters). This paper covers the development of these sensors from 1977 to the present. It describes the operation of interferometric fiber optic sensors including component development and interferometric demodulation techniques; discusses the transduction mechanism from the pressure field to phase modulation in the fiber; and reviews the mechanical design of various sensor configurations including coated fibers and solid and air-backed mandrels. Recent results measured on acoustic sensors employing fibers coated with air-included polymers are presented. The significance of fiber optic sensor multiplexing for use in multi-element arrays is discussed. Finally, a photograph is displayed of the prototype sensors similar to those deployed on the new Virginia Class submarine.

Introduction

Since the first fiber-optic acoustic sensors were reported by Cole et al.¹ and Bucaro et al.² in 1977, their development has continued to advance and is culminating in fleet deployment of these sensor systems.

This paper begins with a description of the operation of fiber optic interferometers and discusses the non-linear response between the optical phase modulation and the intensity output of the interferometer. Methods of linearizing the interferometric output including both feedback and open-loop demodulators are reviewed. The fundamental equation relating strains induced in the core of the optical fiber to the phase modulation of light in the interferometer is presented. Optical fiber wrapped on solid mandrels will be the first fiber interferometric acoustic sensor discussed. Then optical fibers coated with multi-layer polymer coatings and polymer coatings with air-inclusions will be reviewed. As fiber optical interferometric acoustic sensing technology matured, the emphasis changed to multiplexing large number of sensors to form sensor arrays. Several multiplexing configurations are reviewed. Finally, the fiber optic acoustic sensor design used on the USS Virginia is discussed.

Fiber Optic Interferometric Configuration

Figure 1 contains a schematic of a fiber optic Mach-Zehnder interferometer. Any interferometric configuration can be used for these sensors, but a Mach-Zehnder interferometer is convenient for explaining fiber acoustic sensor operation. A laser beam is launched into an optical fiber and is split by a fiber coupler into 2 fibers. The sensing arm is exposed to the acoustic signal while the reference arm is isolated from the signal. Acoustically induced strain in the optical fiber changes the effective optical path through the fiber and therefore phase of the light entering the second coupler relative to the light in the reference arm.

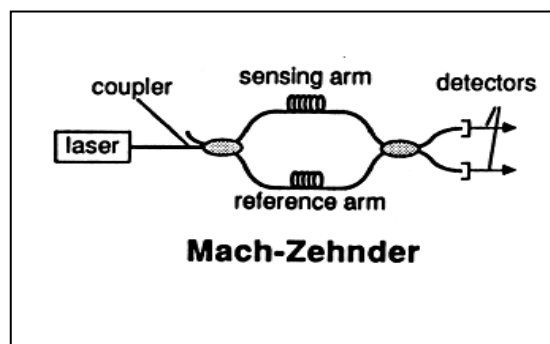


Figure 1. Fiber Optic Interferometer

The normalized output power of the interferometer is plotted as a function of phase in Fig.2. It is clearly seen that the intensity-phase transfer function of the interferometer is non-linear; however, by operating the interferometer at a quadrature bias, as shown by the dot in Fig. 2, a linear response can be obtained for moderate modulation amplitudes. Interferometers are extremely sensitive to thermal variations so feedback was necessary to maintain the quadrature bias point for early sensor measurements. A voltage-controlled phase feedback element was fabricated by wrapping piezoelectric cylinders or discs with optical fiber. Both DC and AC feedback systems were utilized³. It was then determined that non-linear demodulation using synthetic heterodyne⁴ or phase generated carrier⁵ (PGC) demodulation techniques could be employed to allow open loop interferometer operation. Both of these techniques utilize a large phase amplitude carrier applied to the interferometer resulting in the interferometer output containing both a fundamental and second harmonic of the carrier. The acoustic information of interest appears as a sideband around both carriers. As the interferometer slowly drifts, the acoustic signal can always be recovered independently of the bias point. A schematic of a PGC is shown in Fig. 3. This circuit essentially performs the algorithm of $\sin^2 + \cos^2 = 1$. The conception and development of open loop demodulators was critical because they eliminated the requirement for a feedback element for each interferometer, enabling efficient design of multi-sensor arrays.

Fiber Optic Acoustic Transduction

The phase sensitivity of an optical fiber normalized to the total static phase is given by⁶

$$\frac{\Delta\phi}{\phi} = \epsilon_z - \frac{n^2}{2} [(P_{11} + P_{12})\epsilon_r + P_{12}\epsilon_z]$$

where $\Delta\phi$ is the change in phase induced by a change in the strain on the fiber, ϕ is the static phase, n is the index of refraction, P_{ij} are the elasto-optic constants for fused silica and ϵ_z and ϵ_r are the axial and radial strains, respectively. The first fiber interferometric acoustic sensor

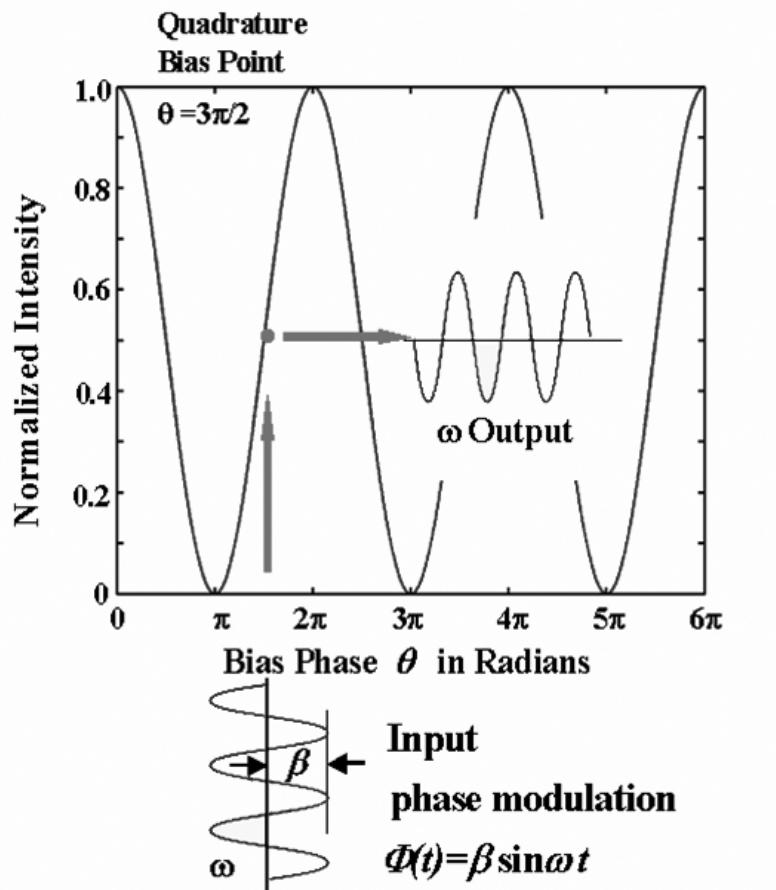


Figure 2. Interferometer Output Intensity

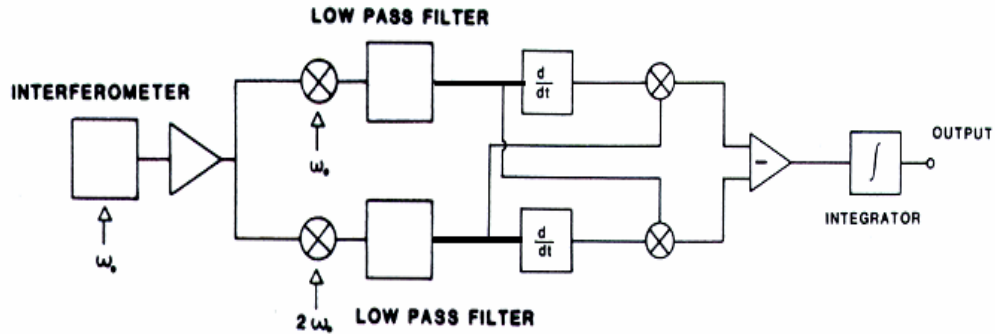


Figure 3. Phase Generated Carrier Demodulator

reviewed is that of an isotropic compliant mandrel, radially wrapped with optical fiber over a portion of its length as shown in Fig. 4A. It is clear that the circumferential change in the mandrel couples directly to a length change in the fiber and therefore to the axial strain, ϵ_z . The first term of Eq.1 for the mandrel case dominates over the second term. The normalized phase sensitivity of the mandrel can be approximated as

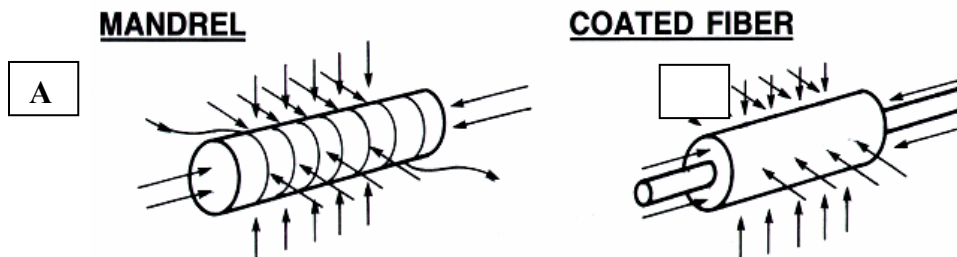


Figure 4. Interferometric Acoustic Transduction Mechanisms

The necessary inclusion of the second term in Eq. 1, is considerably more complicated than the mandrel configuration. Giallorenzi et al.⁷ describe the solution of Eq. 1 using the exact composition and geometry of multi-layer fibers. Utilizing the multi-layer analysis of Reference 7, the stress σ_r , σ_θ , σ_z in cylindrical coordinates is,

$$\begin{bmatrix} \sigma_r^i \\ \sigma_\theta^i \\ \sigma_z^i \end{bmatrix} = \begin{bmatrix} (\lambda^i + 2\mu^i) & \lambda^i & \lambda^i \\ \lambda^i & (\lambda^i + 2\mu^i) & \lambda^i \\ \lambda^i & \lambda^i & (\lambda^i + 2\mu^i) \end{bmatrix} \begin{bmatrix} \varepsilon_r^i \\ \varepsilon_\theta^i \\ \varepsilon_z^i \end{bmatrix}$$

where i is the layer index (0 for the core, 1 for the cladding, etc.) and λ^i and μ^i are the Lamé parameters⁸, which are related to the Young's modulus, E^i , and Poisson's ratio, ν^i , as follows:

$$\lambda^i = \frac{\nu^i E^i}{(1 + \nu^i)(1 - 2\nu^i)}, \quad \mu^i = \frac{E^i}{2(1 + \nu^i)}$$

For a cylinder the strains can be obtained from the Lamé solutions⁵,

$$\varepsilon_r^i = U_0^i + \frac{U_1^i}{r^2}, \quad \varepsilon_\theta^i = U_0^i - \frac{U_1^i}{r^2}, \quad \varepsilon_z^i = W_0^i \quad (4)$$

where, U_0^i , U_1^i , and W_0^i are constants to be determined. Since the strains must be finite at the center of the core, $U_1^0 = 0$. For a fiber with m layers the constants U_0^i , U_1^i , W_0^i in (4) are determined from the boundary conditions

$$\sigma_r^i \Big|_{r=r_i} = \sigma_r^{i+1} \Big|_{r=r_i} \quad (i = 0, 1, \dots, m-1) \quad (5)$$

$$u_r^i \Big|_{r=r_i} = u_r^{i+1} \Big|_{r=r_i} \quad (i = 0, 1, \dots, m-1) \quad (5)$$

$$\sigma_r^m \Big|_{r=r_m} = -P \quad (7)$$

$$\sum_{i=0}^m \sigma_z^i A_i = -PA_m \quad (8)$$

$$\varepsilon_z^0 = \varepsilon_z^1 = \dots = \varepsilon_z^m \quad (9)$$

Where $u_r^i = (\int \varepsilon_r^i dr)$ is the radial displacement in the i th layer, and r_i and A_i are the radius and cross-sectional area of the i th layer, respectively.

Equations 5 and 6 describe radial stress and displacement continuity across the boundaries of the layers. Equations 7 and 8 assume that the applied pressure is hydrostatic. Equation 9 is the plane strain approximation⁹, which ignores end effects. The plane strain approximation assumes that all layers of a composite, multi-layer fiber move together in a single plane when under stress. The plane strain approximation has been shown to be in good agreement with an exact calculation of the axial strain for multi-layer structures¹⁰. Using the boundary conditions described by Eqs. 5-9, the constants U_o^i , U_i^i and W_o^i are determined and ϵ_r^0 and ϵ_z^i are calculated from Eq. 4. Then from Eq. 1 the normalized phase sensitivity, $\Delta\phi/\phi\Delta P$ can be found. The first measurements made with interferometers were made by exposing the optical fiber to the acoustic field^{1,2}. It was observed that polymer coatings on the optical fibers enhanced the acoustic sensitivity. A simple explanation of this phenomenon is that the fiber and coating forms a composite material and that the lower Young's modulus and large cross sectional area of the coating allows greater expansion than the glass fiber and "pulls" the fiber along. Of course this requires good bonding between the optical fiber and the coating. Figure 5 summarizes the Navy's history of the development of acoustically sensitive fiber coatings from the early 1980's to the present. Recently dramatic improvements have been achieved by incorporating air-inclusions within the polymer coating to lower the effect bulk modulus¹¹. This approach is limited to applications at low and moderate static pressures. Ideally, a coated fiber would have adequate sensitivity such that a straight section of fiber would meet the minimum detectable acoustic signal requirements for system applications. Straight fibers demonstrate mechanical resonances, so fiber optic transducers are typically coiled like springs or donuts. This concludes our discussion of the acoustic sensitivity of coated optical fibers; a discussion of mandrel configurations will be continued when we discuss fiber optic acoustic arrays.

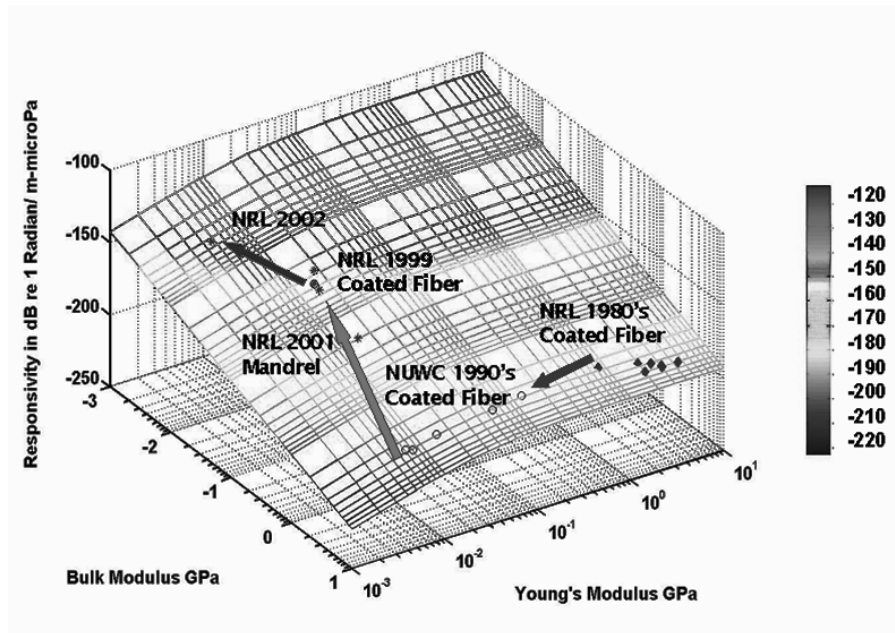


Figure 5: Navy Acoustic Sensor Fiber Coatings History

Component Development

Once the feasibility of fiber optic interferometric detection of acoustic signals was demonstrated, it was necessary to develop the components required to allow interferometers to become field deployable. The first attempt at such a device was the “bottle coupler”¹² which performed the function of an optical beam splitter in a fiber configuration. A drawing and a photograph of a “bottle coupler” are shown in Fig. 6. The polymer coating was removed from two optical fibers and the fibers were epoxied to a bottle such that the exposed section of the glass fibers were twisted around each other. At the top of the bottle the two fibers were epoxied to a threaded cap. A laser and photodetectors were set up to monitor the coupler performance. Buffered hydrofluoric acid was placed into the bottle and the fibers were allowed to etch. (The inside of the bottle also etched, but the thickness of the bottle is much greater than that of the fiber.) When the appropriate amount of coupling was obtained with the buffered solution, the hydrofluoric acid was removed and replaced with index

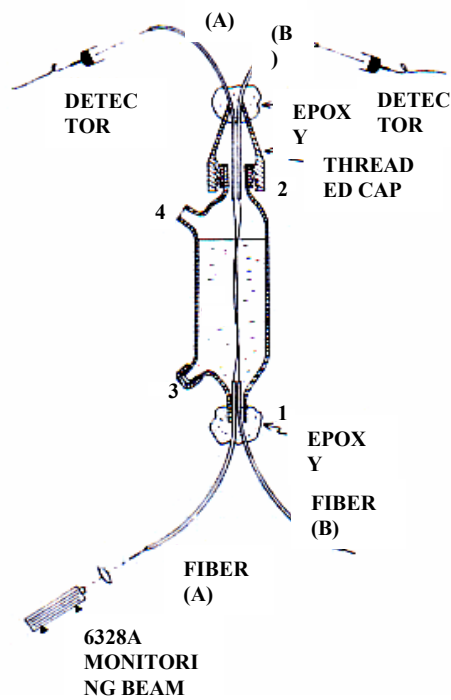


Figure 6. Encapsulated Single Mode Fiber Optical Power Divider

matching fluid. Fine adjustment of the splitting ratio could be accomplished by twisting the cap on the top of the bottle. The splitting ratio of these couplers was somewhat affected by vibration and temperature, but was adequate to demonstrate the first all-fiber interferometer operating as an acoustic sensor. That first all-fiber interferometric acoustic sensor was called the “Glassboard” and results will be presented in the next section.

The difficulty with the bottle couplers was that they were liquid filled and had to stand erect. A next generation of passive fiber optic couplers without the difficulties of the “bottle” couplers had to be

developed. Figure 7. illustrates the configuration of a fused biconical tapered coupler developed by Villarruel and Moeller¹³ at NRL. These NRL couplers were used for the next acoustic sensor demonstration, the “Brassboard”. NRL also sponsored the development of similar fiber optic couplers at Gould leading to the first commercial devices.

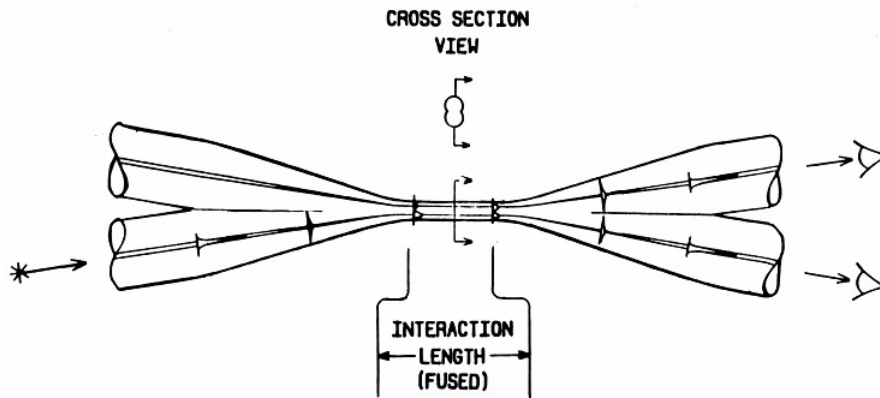


Figure 7. Artist Sketch of a Fused Biconical Tapered Fiber Coupler

Early Acoustic Demonstrations

The measured sensitivity of the “Glassboard”, the first all-fiber interferometer is shown in Fig. 8 plotted as a function of frequency. The left hand axis shows the free field voltage sensitivity in dB re 1 V/ μ Pa, the units associated with a piezoelectric hydrophones. The right hand axis is the optical phase sensitivity in Radians/ μ Pa. Please note that the response is well behaved as a function of pressure but does show some variation with temperature. Figure 9. contains a similar plot for the “Brassboard”

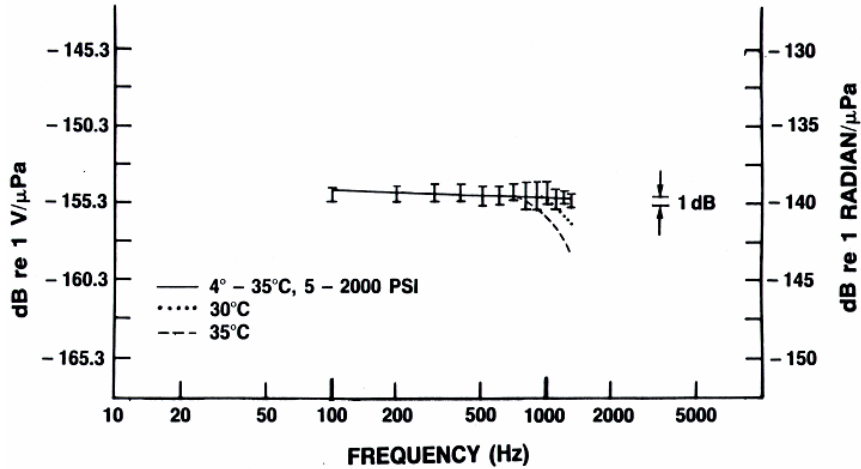


Figure 8. Response of the “Glassboard” Fiber Interferometric Acoustic Hydrophone

fiber optic interferometric hydrophone. The response of the “Brassboard” hydrophone met all acoustic response specifications as a function of both temperature and static pressure. Figure 10. contains plots of the minimum detectable pressure in dB re 1 μPa versus frequency of both the 1980 “Glassboard” and the 1983 “Brassboard” hydrophones. Also plotted are various environmental acoustic noise levels for comparison. By 1983 fiber interferometric acoustic sensors had demonstrated the performance necessary for implementation in Navy acoustic systems. The development of fiber optic couplers was critical to reducing the noise levels of fiber interferometric sensors to the levels shown in Fig.10.

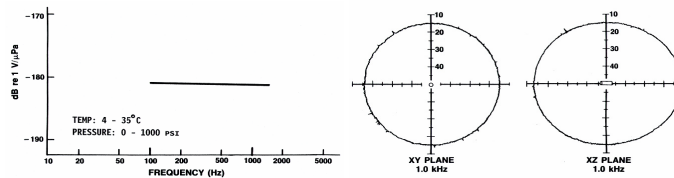


Figure 9. Response and Beam patterns of the “Brassboard”

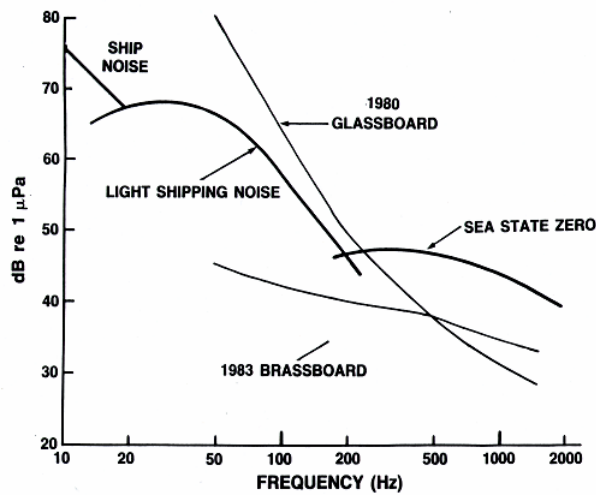


Figure 10. Minimum Detectable Pressure of the “Glassboard” and “Brassboard”

Figure 11 shows a composite plot of the responses of interferometric acoustic sensors of both coated and mandrel configurations plotted as a function of time over 20 years. This figure summarizes the development of mandrel hydrophones from isotropic plastic mandrels discussed above, to air-backed metal and to air-backed plastic mandrels with corresponding increases in performance. Also shown is the development of optical fibers including bare and coated optical fibers. Air-included fiber coatings discussed earlier were demonstrated after 1995 and have not been included in the plot of Fig.11. Many of the hydrophones included in Fig.11 were designed to meet specific demonstration system requirements. Having developed numerous interferometric hydrophone designs, the next task was to demonstrate multi-sensor arrays.

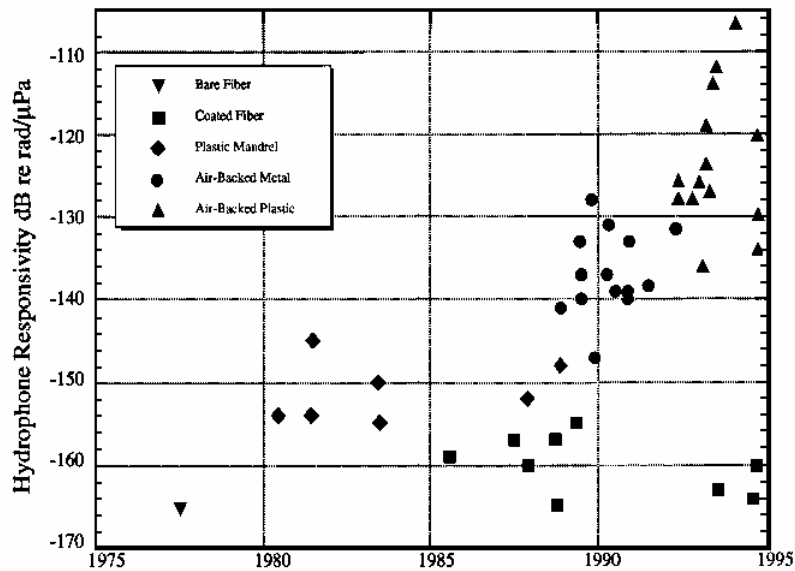


Figure 11. Summary of the Responsivity of Fiber Interferometric Hydrophones

Multi-Element Sensor Array Development

As discussed in Section III. The development of open loop demodulators was critical in the development of multi-element sensor arrays. If feedback techniques are used, a feedback element for each sensor is required. Open loop demodulation enables a single control element to operate many sensors, which comprise an array or a sub-array section. Figure 12. illustrates one configuration, which eliminates the requirement for any active element from a multi-element array enabling totally passive multi-element arrays. When a frequency modulated optical source is input into an interferometer with a pathlength difference between the reference arm and the sensor arm, a phase-generated carrier is created at the frequency of the modulation. The phase modulation, $\Delta\phi = 2\pi\Delta vnl/c$, where Δv is the frequency modulation of the source, n is the index of refraction of the core

of the fiber, l is the pathlength difference between the two arms of the interferometer and c is the speed of light in vacuum. An extension of Fig. 12 to the case of a frequency division multiplexed array¹⁴ of $I \times K$ elements is shown in Fig. 13. Quantity I , multiple phase

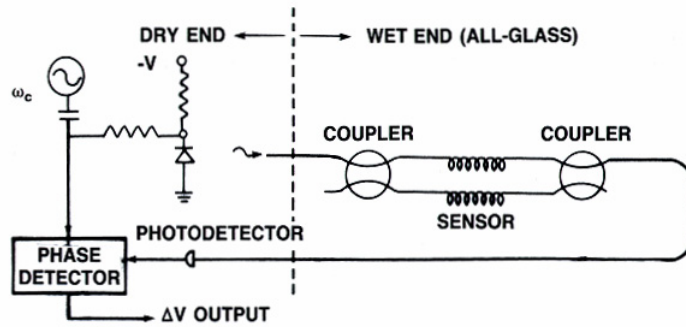


Figure 12. Schematic of a single sensor configuration allowing a totally passive (all glass) deployment

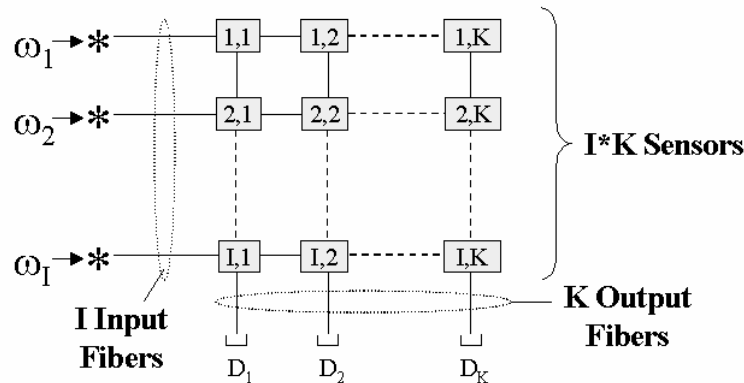


Figure 13. Conceptual schematic of a frequency division multiplexed $I \times K$ array

Generated carrier frequencies ω_i , all at the same optical wavelength, are each input to sub-arrays with K sensors in each array. One sensor from each sub-

array is then multiplexed onto a single output fiber so I+K fibers support I*K sensor elements. It is obvious that different optical wavelengths can be used to extend this concept to arrays with more elements utilizing the same number of fibers. Frequency division multiplexing is used on the new Virginia class submarine. It is important to realize that the frequency division multiplexing described refers to the frequency of the phase-generated carrier not to the optical frequency. Figure 14. illustrates three additional multiplexing techniques. The first technique, frequency/wavelength division

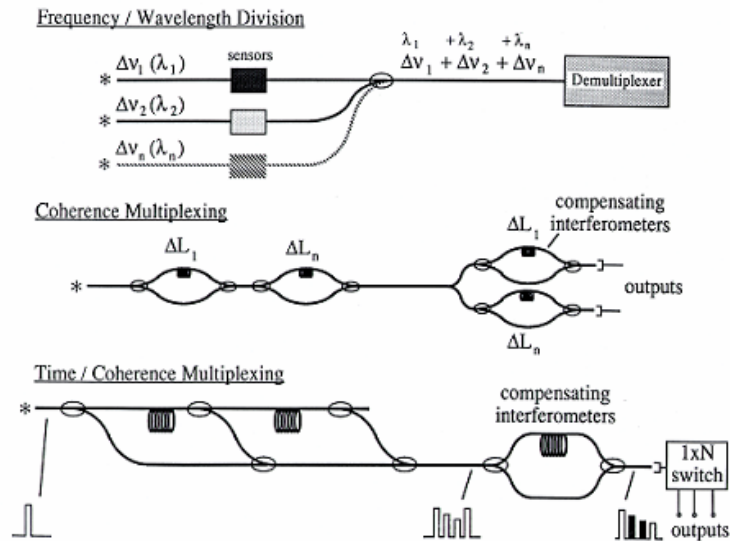


Figure 14. Additional multiplexing configurations

multiplexing¹⁵, refers to employing different optical frequencies/wavelengths in the array rather than different phase generated carriers. Unfortunately this nomenclature can be very confusing since the names are the same but the techniques are totally different and in fact the techniques can be used together to increase array sensor count as was mentioned above.

The second multiplexing technique shown is coherence division multiplexing¹⁶ where each interferometer has a different path delay between the two arms of the interferometer and all the delays are beyond the coherence length of the laser source. The signal from each sensor can be recovered by using an individual compensating interferometer with the path delay from each compensating interferometer matching the corresponding

delay of a sensor. This multiplexing configuration is power inefficient and complex due to the required number of compensating interferometers. The importance of this multiplexing technique is that it forms the basis for the last multiplexing approach shown, time/coherence multiplexing¹⁷. In this case, each sensor interferometer has the same path length delay but a relative difference between adjacent sensors such that a single input pulse generates a separate train of two pulses returning to the compensating interferometer from each sensor. The first pulse in the pulse train from the second interferometer occurs at the same time as the second pulse in the train from the first interferometer. A single compensating interferometer can be used to demultiplex all the sensors of the array. Each of the two sensors and the compensating interferometer has a short and a long path. As shown in the Fig. 14, there are only six possible paths for the pulse to travel since there is no coupling from the short side of the array back to the long side of the array. The first pulse arriving at the output of the compensating interferometer travels the short-short-short path and does not mix with any other pulses. The second pulse consists of two pulses that coherently mix, one pulse travels a short-short-long path while the second pulse travels a long-short-short path. This pulse represents the output of the first sensor. The next pulse travels a long-short-long path and mixes with a pulse that travels a long-long-short path. This pulse represents the output of the second sensor. These pulses are shown as filled in Fig.14. The last pulse exiting the compensating interferometer travels the long-long-long path and does not mix with any other pulses. This approach can be easily extended to include additional sensors.

Combinations and various configurations of time/coherence multiplexing, frequency division multiplexing and wavelength division multiplexing are the primary multiplexing systems used for fiber interferometric acoustic arrays^{18,19}. A combination of time/coherence and wavelength division multiplexing are currently used for demonstrations of systems where high channel counts on low fiber counts, such as bottom mounted arrays, is desired. Frequency division multiplexing is used where higher fiber counts and parallel processing provide higher reliability as in the Virginia Class Submarine.

Figure 15 is a photograph of the fiber optic interferometric hydrophone used on the submarine. The photo appears to be blurred due to the material encapsulating the fiber coils.

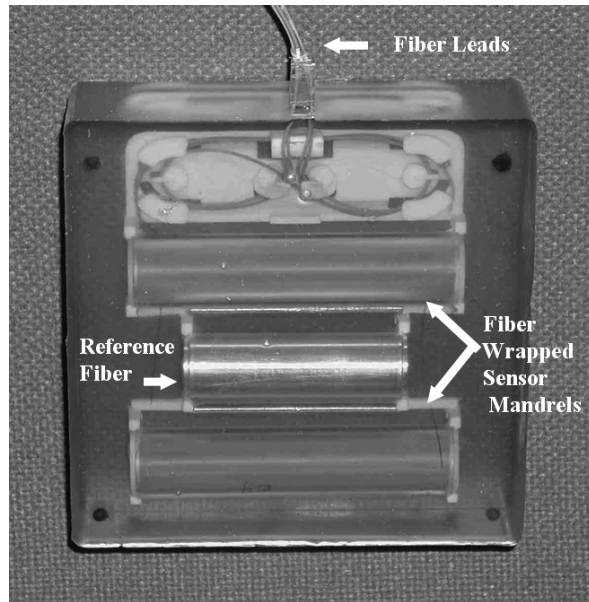


Figure 15. Virginia Class Fiber Optic Hydrophone

Conclusions

This paper has provided an overview of the development of interferometric fiber optic acoustic sensors over the past 25 years at the Naval Research Laboratory. The interested reader can use the references provided to develop a more comprehensive understanding of this technology.

References

- ¹J. H. Cole, R. L. Johnson and P. G. Bhuta, "Fiber Optic Detection of Sound", *J. Acoust. Soc. Amer.* vol. 62, p. 1136, 1977
- ²J. A. Bucaro, H. D. Dardy and E. F. Carome, "Fiber Optic Hydrophone", *J. Acoust. Soc. Amer.* vol. 62, p. 1302, 1977
- ³I.J. Bush, "A synchronous Phase Detection System for an Optical Interferometric Sensor", *NRL Memorandum Report 4808*, 1982
- ⁴James H. Cole, Bruce A. Danver and Joseph A. Bucaro, "Synthetic-Heterodyne Interferometric Demodulation" *IEEE JQE.* vol. QE-18, p. 694, 1982

-
- ⁵Anthony Dandridge, Alan B. Tveten and Thomas Giallorenzi, "Homodyne Demodulation Scheme for Fiber Optic Sensors Using Phase Generated Carrier", IEEE JQE. vol. QE-18, p. 1647, 1982
- ⁶J. A. Bucaro, N. Lagakos, J.H. Cole and T.G. Giallorenzi," Fiber Optic Acoustic Transduction", Edited by Warren P. Mason and R.N. Thurston, Chapter 7, PHYSICAL ACOUSTICS, XVI, p. 385, (Academic Press) 1982
- ⁷Thomas G. Giallorenzi, Joseph A. Bucaro, Anthony Dandridge, G.H. Sigel, Jr., James H. Cole, Scott C. Rashleigh and Richard G. Priest, "Optical Fiber Sensor Technology", IEEE JQE. vol. QE-18, p. 626, 1982
- ⁸S.P. Timoshenko and J.N. Goodier, Theory of Elasticity (McGraw-Hill, NewYork, 1970), Chap. 4.
- ⁹B. Budiansky, D.C. Drucker, G.S. Kino, and J.R. Rice, "Pressure sensitivity of a clad optical fiber", Appl. Opt. vol.18, p. 4085, 1979
- ¹⁰R. Hughes and J. Jarzynski, "Static pressure sensitivity amplification in interferometric fiber-optic hydrophones", Appl. Opt. vol. 19, p. 98, 1980
- ¹¹James H. Cole, Sara Motley, Jacek Jarzynski, Alan B. Tveten, Clay Kirkendall and Anthony Dandridge, "Air-Included Polymer Coatings for Enhanced Sensitivity of Fiber-Optic Acoustic Sensors", Technical Digest, 16th Optical Fiber Sensors Conference, p. 214, 2003
- ¹²S. K.Sheem and T.G. Giallorenzi, "Single Mode Fiber Optical Power Divider: Encapsulated Etching Technique", Opt. Lett. vol. 4 p. 29, 1979
- ¹³C.A. Villarruel and R.P. Moeller, Fused Single Mode Fibre Access Couplers", Elect. Lett. vol. 17, p. 243, 1981
- ¹⁴A. Dandridge, A.B. Tveten, A.M. Yurek, A.D. Kersey, and E.C. McGarry, 'Frequency Division Multiplexing of Interferometric Sensor Arrays', NRL Memorandum Rpt., No. 6457, (1989)
- ¹⁵A. D. Kersey and A. Dandridge, 'Comparative Analysis of Multiplexing Techniques for Interferometric Fiber sensors', SPIE, vol. 1120, p. 236, 1989
- ¹⁶R. H. Wentworth, 'Theoretical Noise Performance of Coherence-Multiplexed Interferometric Sensors', J. Lightwave Technol., vol. 7, p. 941, 1989
- ¹⁷A. D. Kersey, A Dandridge, and A. B.Tveten, 'Time-division multiplexing of Interferometric fiber sensors using passive phase-generated carrier interrogation', Optics Lett., vol. 12, p. 775, 1987
- ¹⁸A.R. Davis, C.K. Kirkendall, A. Dandridge, and A.D. Kersey, "64 Channel All Optical Deployable Acoustic Array" in Proc OFS, vol. 12, p. 616, (1997)
- ¹⁹G.A. Cranch, C.K. Kirkendall, K. Daley, S. Motley, A. Bautista, J. Salzano, P.J. Nash, J. Latchem, and R. Crickmore, "Large-Scale Remotely Pumped and Interrogated Fiber-Optic Interferometric Sensor Array", IEEE Photonics Technology Letters, vol. 15, p.1579, 2003